*Geophys. J. Int.* (1999) **138,** 343–352

# Residence time of diffuse waves in the crust as a physical interpretation of coda $Q$: application to seismograms recorded in Mexico

L. Margerin,[1] M. Campillo,[1] N. M. Shapiro[2] and B. van Tiggelen[3]

[1] *Laboratoire de Géophysique Interne et Tectonophysique, Observatoire de Grenoble, Université Joseph Fourier,* BP 53, 38041 *Grenoble Cedex, France. E-mail: lmarger@obs.ujf-grenoble.fr*

[2] *Instituto de Geofísica, Universidad Nacional Autonoma de México, CU,* 04510 *México, DF, Mexico*

[3] *Laboratoire de Physique et Modélisation des Systèmes Condensés, Maison des Magistères Jean Perrin, CNRS,* BP 66, 38042 *Grenoble Cedex, France*

Accepted 1999 February 22. Received 1999 February 5; in original form 1998 June 22.

## SUMMARY

We consider a simple model for elastic wave propagation in the Earth's lithosphere consisting of a heterogeneous and scattering crust overlying a homogeneous mantle; that is, we neglect backscattering from the upper mantle. This rough condition is not strictly valid everywhere, but this model allows us to investigate the effects of variations of diffracting properties between crust and mantle on the coda decay. The free parameters describing the wave propagation are the mean free path of the waves and the intrinsic absorption in the crust. In the framework of the radiative transfer theory, we treat, accurately, jumps in $S$-wave speed and the mean free path at the Moho. Without intrinsic absorption, this configuration yields a synthetic coda decay $1/t\exp(-2\pi ft/Q_c^*)$, a form similar to that proposed by Aki & Chouet (1975) to parametrize the observations. The exponential decay in our purely elastic model is due to the partial leakage of diffuse energy into the mantle.

In order to test the applicability of our model, we have determined the coda $Q$ parameter ($Q_c$) in the 1–15 Hz frequency band from data recorded at four stations in Mexico. In the low-frequency regime (around 1 Hz), we suggest that the energy leakage significantly affects coda $Q$, whilst at higher frequencies (around 10 Hz), the anelastic attenuation dominates. A weak intrinsic absorption expressed by a frequency-independent parameter, $Q_i$, of about 1000 accounts satisfactorily for the observed $Q_c$ values in the whole frequency range. Our very simple model has only two free parameters and offers an attractive alternative physical interpretation of coda $Q$. In Mexico, this model is sufficient to interpret the coda observations.

According to our model, in regions where the mean free path is much larger than the crustal thickness (weakly heterogeneous crust), the leakage effect should be small, and the observed $Q_c$ will mainly be due to the intrinsic absorption. On the other hand, when the mean free path is of the order of the crustal thickness (strongly heterogeneous crust), we predict a strong sensitivity of the decay rate of the coda to the crustal thickness. This dependence may be important for the interpretation of the regional variations of coda $Q$. We propose introducing a new parameter, $\tau_d$, the residence time of diffuse energy in the crust, which is physically more meaningful than a quality factor to quantify the leakage effect.

**Key words:** coda, diffusion, multiple scattering, $Q$, radiative transfer.

## 1 INTRODUCTION

Since coda waves were first recognized as scattered waves on randomly distributed inhomogeneities in the lithosphere (Aki 1969; Aki & Chouet 1975), seismologists have tried to deduce a statistical parameter describing the scattering in the lithosphere from coda records (that is, the mean free path of the waves, $l$), as well as the intrinsic absorption of rocks, $Q_i$. Due to the complexity of elastic wave propagation in the lithosphere, some simplifications had to be introduced regarding the physical processes and/or the mechanical and scattering properties of the Earth. The early interpretation of the coda as singly scattered waves in a uniform infinite space led to several estimates of the mean free path of waves (see Herraiz & Espinosa 1987 for a review). However, higher scattering orders may not be negligible, and several attempts have been made to include multiple scattering. For example, Wu & Aki (1988), Fehler *et al.* (1992) and Hoshiba (1993) developed different methods, all based on radiative transfer theory in a uniform half-space, to estimate the mean free path of waves and seismic albedos. However, as pointed out several times in the literature (e.g. Abubakirov & Gusev 1990; Fehler *et al.* 1992; Hoshiba 1993), the underlying assumption that the Earth is homogeneous with regard to wave speeds and mean free paths is known to be inaccurate. In the following, we present a new simplified model of scattering in the Earth that incorporates the Moho at depth, the free surface and a heterogeneity contrast between crust and mantle. By analysing a specific set of data from Mexico, we demonstrate that the present model accounts for the frequency dependence of coda $Q$ in this region.

## 2 PRESENTATION OF THE MODEL

We consider a conceptual model consisting of a heterogeneous and scattering crust with low $S$-wave velocity overlying a homogeneous and weak scattering mantle with high $S$-wave velocity. The velocity contrast between crust and mantle is well documented. The heterogeneous character of the crust is known from geological observations as well as from deep seismic soundings. Deep reflection seismology offers direct access to the depth dependence of the reflection/diffraction properties in the crust and mantle beneath the continents. The frequency band used in these experiments (typically 5–20 Hz) overlaps widely that of coda studies (1–20 Hz). The results of the deep reflection experiments are therefore relevant to the description of the structures associated with scattering in the lithosphere. A considerable effort has been invested worldwide to provide seismic images of the deep crust. The programmes COCORP in the USA, BIRPS in Britain, DEKORP in Germany, LITHOPROBE in Canada, BABEL in Fennoscandia and ECORS in France, amongst others, have confirmed general features in the seismic picture of the continental lithosphere [see e.g. Allmendinger *et al.* 1987; Meissner 1989; contributions to the Proceedings of the 4th International Symposium on Deep Reflection Profiling of the Continental Lithosphere (Meissner *et al.* 1990 )]. A striking characteristic of the continental lithosphere revealed by deep reflection experiments is the strong variation of the seismic reflectivity observed in different regions of the world at a depth corresponding to the Moho. Above the Moho, the lower crust is reflective, whilst below the Moho the upper mantle is generally almost transparent. The Moho can even be defined on these sections as the deepest limit of the reflective crust. The crustal reflectivity depends strongly on the geological setting (Allmendinger *et al.* 1987; Meissner 1989). There are some examples of reflectors below the Moho (McGeary & Warner 1985; Cloves *et al.* 1996; Krishna *et al.* 1996), but they are exceptional. Nevertheless, these sub-Moho reflections demonstrate the ability of the soundings to probe the upper mantle. The huge amount of observations that have been obtained by the deep reflection programmes cannot be overlooked in the construction of simple models of heterogeneity in the lithosphere.

Based on the results of studies of pulse broadening (Abubakirov & Gusev 1990) and analyses of coda decay, Gusev (1995) invoked a strong variation of scattering strength with depth and claimed the potential importance of this layering for the interpretation of coda $Q$. Consequently, our model, whose characteristics are shown in Fig. 1, is not just an *ad hoc* model since numerous seismological and non-seismological arguments have led us to study such a simple configuration. We do not expect our model to represent the actual structure of the lithosphere in every region of the world. Aki (1980a,b) measured the attenuation of direct $S$ waves for earthquakes above and below the Moho beneath Japan and found results that suggest only a very weak increase of $l$ with depth. Despite its simplicity, our model introduces new features in the study of coda waves, namely the existence of a velocity and mean free path contrast at a certain depth. We model multiple scattering using an acoustic radiative transfer equation supplemented by appropriate boundary conditions. In our analysis, mode conversions are neglected, and isotropic scattering is assumed, whilst the angular dependence of transmission and reflection coefficients of acoustic energy at the Moho is taken into account. We consider mean free path values covering one order of magnitude, from 10 to 100 km. The relevance of these values will be demonstrated in the data interpretation section of this paper. The way to deal with a reflective interface as well as depth-dependent mean free path values has been described in a previous paper (Margerin *et al.* 1998, hereafter referred to as Paper I; see also Hoshiba 1997). An important feature of our model is the partial leakage of energy at the base of the crust into the mantle, which gives a functional form of the synthetic coda decay very different from the decay obtained in uniform models without anelasticity. This point is discussed in detail in the next section.

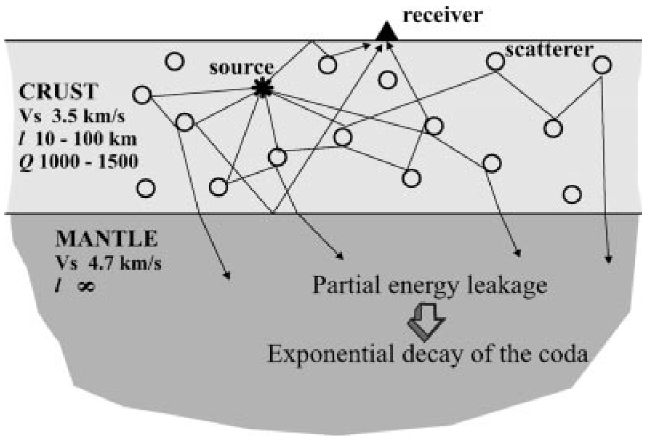


**Figure 1.** Geometry and physical parameters of the model.

## 3 DESCRIPTION OF SYNTHETIC CODA

First, we consider a model without intrinsic absorption. In Paper I, we presented a series of Monte-Carlo solutions of the radiative transfer equation for the lithospheric model discussed above. These numerical tests have shown that for a large range of mean free path values (from 10 to 100 km), the envelope of the synthetic coda in the multiple scattering regime follows the formulae

$$\rho(t) = \frac{1}{t}\exp\left(-\frac{t}{\tau_{\rm d}}\right), \tag{1}$$

$$\tau_{\rm d} = \frac{Q_{\rm c}^*}{2\pi f}, \tag{2}$$

where $\rho$ is the energy density in the coda, $t$ the time elapsed since the energy release at the source, $f$ the wave frequency, $Q_{\rm c}^*$

the parameter that describes the decay rate of our model, and $\tau_d$ the characteristic residence time of diffuse waves in the crust, which measures the rate of leakage into the mantle.

We denote by $Q_0^*$ the value of $Q_c^*$ at the frequency $f=1$ Hz. Formula (1) shows the same functional form as that proposed by Aki & Chouet (1975) to measure coda $Q$, a parameter extensively used to describe the decay rate of actual seismogram envelopes. This analogy with the classical quality factor is somewhat arbitrary, but justified by its wide application in seismology. Physically, we believe that a residence time of energy is more meaningful to characterize the leakage effect. This will be discussed in the last section.

The physical interpretation of eq. (1) is as follows (Paper I). The $t^{-1}$ dependence corresponds to the asymptotic decay associated with a diffusion process without absorption in a 2-D medium. The exponential factor expresses the energy loss into the mantle due to the waves that reach the Moho below the critical angle. We have shown in Paper I that for mean free paths smaller than the crustal thickness and sufficiently large lapse times, the radiative transfer equation is basically equivalent to a diffusion equation that can be solved analytically. This provides closed-form expressions of $Q_0^*$ in terms of the physical parameters of the model,

$$l < H: \begin{cases} Q_0^* \simeq \dfrac{2\pi H^2}{D\xi^2} \simeq \dfrac{6\pi H^2}{vl\xi^2} \\ \tau_d \simeq \dfrac{H^2}{D\xi^2} \simeq \dfrac{3H^2}{vl\xi^2} \end{cases}, \qquad (3)$$

where $H$ is the thickness of the crust, $D$ the diffusion constant of waves, $v$ the $S$-wave speed, and $\xi$ a parameter representing the effect of internal reflection at the Moho, dependent on the mean free path and the crustal thickness. The mean free path, $l$, and $D$ are related by $D=vl/3$. Note that $\xi \in ]0, \pi/2[$ and that the frequency $f=1$ Hz is implied in the definition of $Q_0^*$. This formula, whilst restricted to the domain of validity of our diffusion approximation, helps to clarify the physics of the leakage process. On the basis of eq. (3), we conclude that the larger the diffusion constant, the faster the diffuse energy leaks into the mantle. We note that the crustal thickness $H$ affects the leakage rate even more than the mean free path, since $Q_0^*$ and $\tau_d$ increase with the square of $H$ (see eq. 3). We emphasize that the analytical relation between $Q_0^*$, $l$ and $H$ is restricted to the domain of validity of the diffusion approximation ($l < H$). In particular, one should not extrapolate eq. (3) to values of the mean free path larger than the crustal thickness.

Outside the domain $l < H$, the diffusion approximation no longer describes the partial trapping of waves in the crust, mainly because it assumes a nearly isotropic field and angularly averaged values of the reflection coefficient at the Moho. As the mean free path in the crust increases, post-critical reflections at the Moho contribute more and more to the energy trapped in the crust, which is not described properly in our diffusion approximation. Therefore, to quantify the leakage effect for $l > H$, we must rely on the radiative transfer theory, which provides a complete framework, where the angular dependence of the internal reflection at the Moho is accurately taken into account. Surprisingly, it turns out that expression (1) holds true even outside the restrictive domain where our analytical solution of the diffusion equation is justified. In Fig. 2 we present the numerical solutions of the radiative transfer equation. Earthquakes are assumed to be very shallow and the receivers are located on the free surface near the source. These assumptions are made for simplicity but are by no means necessary. In particular, the leakage rate does not depend on the source position in the crust, as long as the source–station distance is smaller than a few mean free paths. In Fig. 2 we have also plotted the approximations of the numerical solutions given by expression (1), where the values of $Q_0^*$ were determined by a simple regression. For the different crustal thicknesses and mean free path values considered, we note that for lapse times larger than 20 s, formula (1) fits the numerical solution very closely. We conclude that when $l > H$, the functional dependence (1) is still accurate but $Q_0^*$ has to be evaluated numerically.

Calculations have been performed for three different thicknesses, $H=20$, 30 and 40 km, and mean free paths ranging from 10 to 100 km. The dependence of $1/Q_0^*$ is plotted as a function of the mean free path in Fig. 3 for the three different values of $H$. We note that when $l < H$, $1/Q_0^*$ (or $1/\tau_d$) increases with $l$ according to formula (3). When $l$ is of the order of or larger than $H$, $1/Q_0^*$ decreases as $l$ increases, because in this case the leakage rate is governed by the number of scatterings per unit time. Scattering causes the loss of trapped energy into the mantle, but with increasing $l$ the number of scattering events decreases. We note that in the two cases $l \ll H$ and $l \gg H$, the leakage effect is small, as shown in Fig. 3. As a consequence, when $l$ is much larger than $H$, $Q_0^*$ is large and almost independent of the value of $H$. On the other hand, when $l$ is of the order of $H$, $Q_0^*$ strongly decreases with $H$ (see Fig. 3).

Although extreme, our assumption of a transparent mantle does not represent a singular case with respect to models where the mean free path is much larger in the mantle than in the crust. In Fig. 4 we present the results of simulations of the radiative transfer equation in stratified models with increasing values of mean free paths in the mantle. These computations show the progressive evolution of the shape of the curves from the uniform case to the case of a transparent mantle. When the mean free path is much larger in the mantle than in the crust, our former conclusions are not qualitatively altered.

The question we want to address next is the importance of the leakage for the interpretation of observed coda and the estimation of the mean free path and intrinsic absorption in the crust. This will be studied by applying our model to account for the frequency dependence of coda $Q$ measured in Mexico.

## 4 OBSERVATIONS

We consider a data set of 45 local earthquakes (maximum epicentral distance less than 50 km) recorded at stations CAIG, HUIG, PNIG and ZIIG of the Mexican broad-band network (Singh *et al.* 1997). The earthquake locations and magnitudes are given in Table 1 and the epicentres are plotted in Fig. 5. CAIG, HUIG, PNIG and ZIIG are located along the Mexican coast, where the crust is possibly 30 km thick (Kostoglodov *et al.* 1996). In fact, the crustal thickness is not perfectly determined in that region and we will assume an average crustal thickness ranging from 20 to 30 km, since the crust is expected to become thinner in the direction of the ocean. We measure the time decay of the coda using the procedure outlined by Aki & Chouet (1975). The noise level is observed before the onset of the first arrival. We end the coda analysis when the signal becomes smaller than four times the noise level. The analysis starts about 30 s after the first $S$-wave

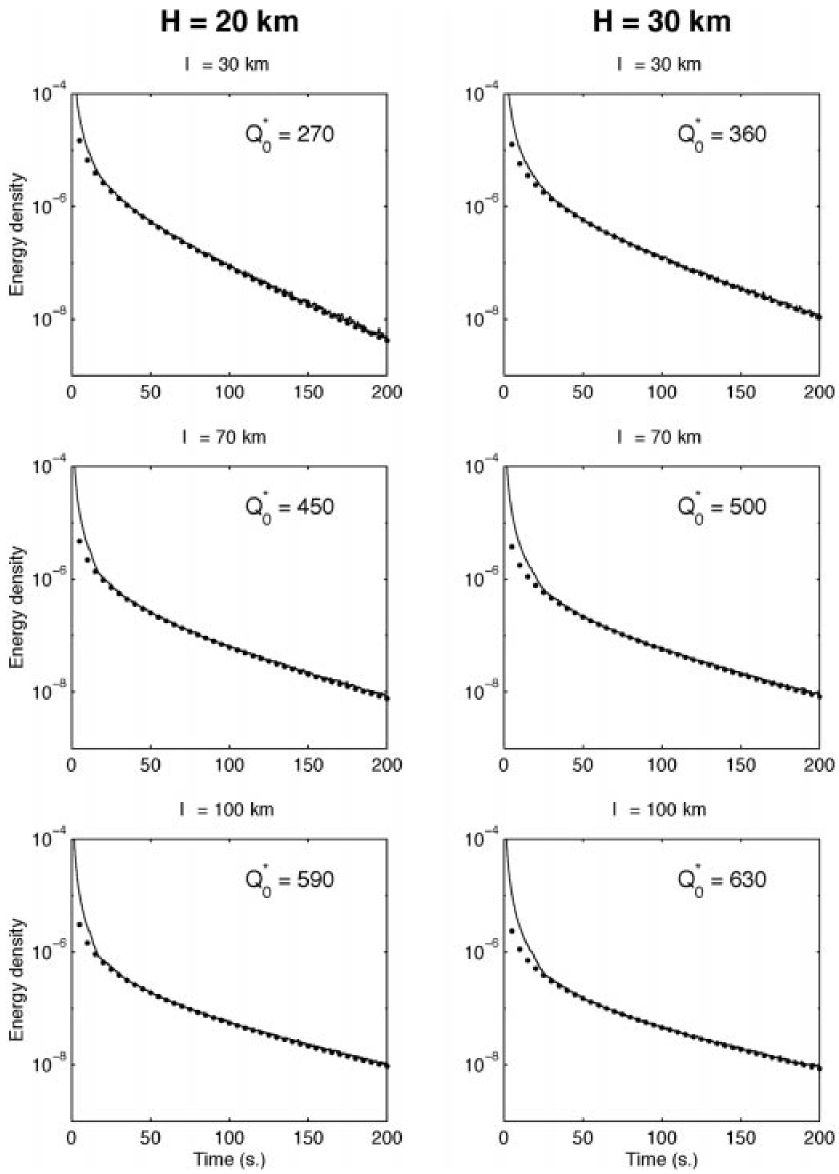


**Figure 2.** Coda decay obtained for our model with $H=20$ and 30 km and the mean free path of the crust $l$ ranging from 30 to 100 km. Solid lines show the numerical solution of the radiative transfer equation and dotted lines show the best approximation obtained with the formula $(1/t)\exp(-2\pi t/Q_0^*)$. The $Q_0^*$ value corresponding to the best approximation is given in the figures. The maximum standard deviation of the $Q_0^*$ is $\Delta Q_0^* \approx 30$.

arrival, which roughly corresponds to the time when the signals exhibit a steady decay. The signal is bandpass filtered in a frequency window with a width of 2/3 the central frequency. The energy of the signal is calculated in half-overlapping time windows of duration three times the central period of the signal. By squaring the amplitude time-series and then summing the values in a time window, an intensity time-series $E_k^i$ is obtained, where $i$ denotes the $i$th record and $k$ the $k$th point in time, and the origin time is the energy release at the source.

The envelopes have been assumed to follow the relation

$$\log(E_k^i {t_k^i}^n) = A^i - \frac{2\pi f t_k^i}{Q_c}\,. \tag{4}$$

The $A^i$ are individual amplitudes of the envelopes, $Q_c$ is the coda $Q$ parameter common to the set of envelopes, and $n$ is an exponent depending on the model used for interpretation. It equals 2 for the single scattering of body waves (see Aki & Chouet 1975) and 1 in our model. The best solution in the least-squares sense of the system of linear equations (4) has been determined by the singular value decomposition method. The statistics on about 10 events at each station give stable $Q_c$ values that are not significantly modified by adding or suppressing one event to or from the set we have used. The fit was made for both $n=1$ and $n=2$. The exponent $n=1$ gives the smallest relative error (about 2 per cent) on the $Q_c$ values, whilst the error reaches 4 per cent for $n=2$. In Fig. 6 we show an example of smoothed coda envelopes and the fit obtained using our model. The central frequency of the signals is 3 Hz and the measured $Q_c \approx 570$. From Fig. 6 it is apparent that the whole coda is fitted satisfactorily with a time-independent $Q_c$.

**Table 1.** Locations and magnitudes of earthquakes used in this study.

Station CAIG

| Latitude | Longitude | Depth (km) | Magnitude |
|---|---|---|---|
| 16.81 | −100.23 | 7.0 | 4.6 |
| 16.82 | −100.25 | 1.0 | 4.6 |
| 16.87 | −100.27 | 15.0 | 4.7 |
| 17.37 | −100.30 | 7.0 | 4.8 |
| 16.81 | −99.81 | 6.0 | 4.9 |
| 16.82 | −100.42 | 21.0 | 4.6 |
| 16.87 | −99.92 | 9.0 | 4.2 |
| 16.97 | −100.75 | 20.0 | 4.5 |
| 17.07 | −100.23 | 23.0 | 4.2 |
| 16.52 | −100.05 | 22.0 | 4.6 |

Station HUIG

| Latitude | Longitude | Depth (km) | Magnitude |
|---|---|---|---|
| 15.38 | −96.56 | 20.0 | 4.7 |
| 15.878 | −96.39 | 0.0 | 4.6 |
| 15.891 | −96.28 | 0.1 | 4.5 |
| 15.606 | −96.51 | 17.4 | 4.5 |
| 15.714 | −96.15 | 49.8 | 4.2 |
| 15.804 | −96.43 | 10.0 | 4.3 |
| 15.690 | −96.48 | 17.3 | 5.0 |
| 15.731 | −96.48 | 3.7 | 4.5 |
| 15.40 | −95.79 | 20.0 | 4.9 |
| 15.86 | −95.89 | 36.0 | 4.8 |
| 16.15 | −96.08 | 15.0 | 4.4 |
| 15.83 | −95.81 | 9.0 | 4.2 |

Station PNIG

| Latitude | Longitude | Depth (km) | Magnitude |
|---|---|---|---|
| 16.34 | −98.49 | 84.0 | 4.6 |
| 16.56 | −98.51 | 13.0 | 4.5 |
| 16.34 | −98.13 | 8.0 | 4.2 |
| 15.96 | −98.00 | 20.0 | 4.0 |
| 16.32 | −98.62 | 5.0 | 5.0 |
| 16.24 | −98.29 | 5.0 | 5.6 |
| 16.26 | −98.25 | 7.0 | 4.4 |
| 16.38 | −98.50 | 21.0 | 5.5 |
| 15.92 | −98.00 | 29 | 4.7 |
| 16.01 | −98.29 | 5.0 | 4.7 |
| 16.04 | −98.04 | 5.0 | 4.5 |

Station ZIIG

| Latitude | Longitude | Depth (km) | Magnitude |
|---|---|---|---|
| 17.15 | −101.14 | 15.0 | 4.5 |
| 17.49 | −101.14 | 18.0 | 6.5 |
| 17.33 | −101.40 | 20.0 | 4.9 |
| 17.31 | −101.16 | 20.0 | 4.1 |
| 17.52 | −101.20 | 30.0 | 5.3 |
| 17.29 | −101.50 | 5.0 | 4.7 |
| 18.05 | −101.57 | 70.0 | 4.4 |
| 17.11 | −101.28 | 4.0 | 5.6 |
| 17.210 | −101.34 | 14.3 | 4.4 |
| 17.366 | −101.49 | 5.0 | 4.4 |
| 17.23 | −101.33 | 5.0 | 4.9 |
| 17.26 | −101.17 | 24.0 | 5.6 |

## 5 DATA MODELLING AND INTERPRETATION

In this section we explain using a specific example (station CAIG) how our results can be applied to model the frequency dependence of coda $Q$. We then show that our model can be used to explain globally the measurements of coda $Q$ along the Pacific coast of Mexico. The measurements of $1/Q_c$ with respect to the frequency at CAIG are plotted in Fig. 7 with error bars. The dashed curves in Fig. 7 limit the domain of $1/Q_c^*$ obtained in our purely elastic model for thicknesses of 20 and 30 km. Since we cannot say *a priori* how $l$ varies with frequency, we assume that for $1\ \mathrm{Hz} \leq f \leq 15$ Hz, we have $20\ \mathrm{km} < l(f) < 100$ km. We exclude smaller mean free path values because they would lead to unrealistic attenuation of the primary $S$ wave.

When $l$ is assumed to be frequency-independent, the parameter $Q_c^*$ is of the form $Q_0^* f$ (that is, $\tau_d$ is independent of the frequency) because $l$ is the only parameter that may depend on frequency in our model. In some simple cases, it may be possible to determine the frequency dependence of the mean free path. For example, let us introduce the correlation length of the fluctuations in the medium $a$, and the wavelength $\lambda$. In the low-frequency limit ($\lambda \gg a$), the mean free path varies as $f^{-4}$, whereas in the high-frequency limit ($\lambda \ll a$), $l$ varies as $f^{-2}$. If the medium is self-similar and contains all length scales of inhomogeneities, one may expect $l$ to be weakly frequency-dependent. It is beyond the scope of this paper to discuss more complicated cases that may occur in the lithosphere. When $1/Q_c^*$ is plotted as a function of frequency for the two limiting values $l = 20$, 100 km, one obtains the two branches of a hyperbola shown in Fig. 7 limiting the estimated variation of the parameter $1/Q_c^*$.

Around 1 Hz, the values of coda decay predicted for a purely elastic model are of the same order as those measured on actual data. This shows that the value of $1/Q_c$ measured at 1 Hz can possibly be explained by the leakage effect without invoking any intrinsic absorption. If we had neglected the leakage effect, as is the case in uniform half-space models, we would have been obliged to ascribe the value of $1/Q_c$ to the intrinsic attenuation in the crust around 1 Hz. At higher frequencies, we see in Fig. 7 that the leakage effect becomes negligible with respect to the anelastic absorption. We can expect that, in the high-frequency limit, $Q_c$ gives an estimate of the anelastic absorption in the crust. We also point out that, when the leakage is dominant, the notion of 'coda quality factor' tends to lose its physical meaning. We find it more natural to use a characteristic time $\tau_d^*$, such that the coda decays as $1/t \exp(-t/\tau_d^*)$. The new parameter, $\tau_d^*$, represents the typical time necessary for the diffuse energy partially trapped in the crust to escape into the mantle.

In order to fit the frequency dependence of $Q_c$ in the entire frequency band, we have to take into account the intrinsic attenuation of rocks. Thus, we introduce in the model an intrinsic quality factor, $Q_i$. In a first step, $Q_i$ is assumed to be frequency-independent. We will discuss the implications of this assumption in the case of the Mexican data. We note that frequency-independent quality factors of about 1500 have been measured for $L_g$ waves in the 1–20 Hz frequency band in stable shield areas, where scattering is expected to be very weak (Hasegawa 1985). We use this measurement as a typical order of magnitude of the intrinsic quality factor for dry crustal rocks. We define the total attenuation predicted by the model as $1/Q_m^* = 1/Q_i + 1/Q_c^*$. In Fig. 8 we present a comparison between the observations at CAIG and the model predictions including intrinsic absorption. For crustal thicknesses of 20 and 30 km and intrinsic $Q$ ranging from 1100 to 1200, the model expectations are in good agreement with the observations in the whole frequency range. We do not aim to find a 'best' set of

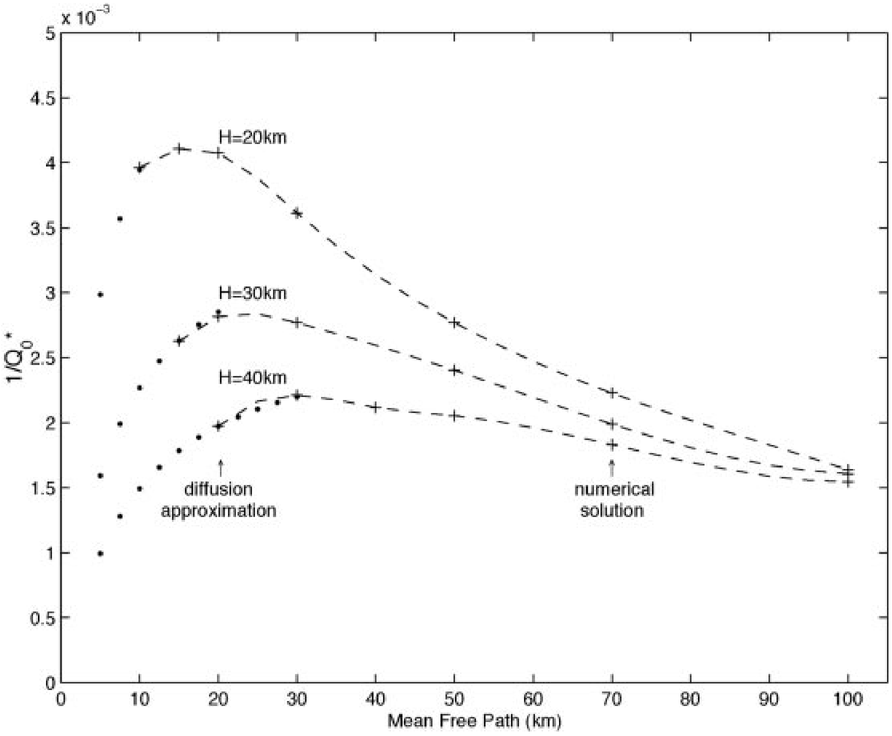


**Figure 3.** Dependence of the parameter $1/Q_0^*$ on the mean free path $l$ for three crustal thicknesses, $H=20$, 30 and 40 km. Dots correspond to the values calculated with the diffusion approximation and crosses denote the values estimated numerically with the radiative transfer theory. Both coincide for $l < H$. The dashed lines interpolate between the crosses.

model parameters; rather, we would like to capture the relative importance of the physical processes at work. The data are fitted satisfactorily with only two free parameters, $l$ and $Q_i$, both with very reasonable values. Therefore, our data set does not require us to introduce an *ad hoc* strong frequency dependence of $Q_i$. In Fig. 9 we present the measurements carried out at four stations along the Pacific coast. The observations exhibit the same main features. For the two crustal

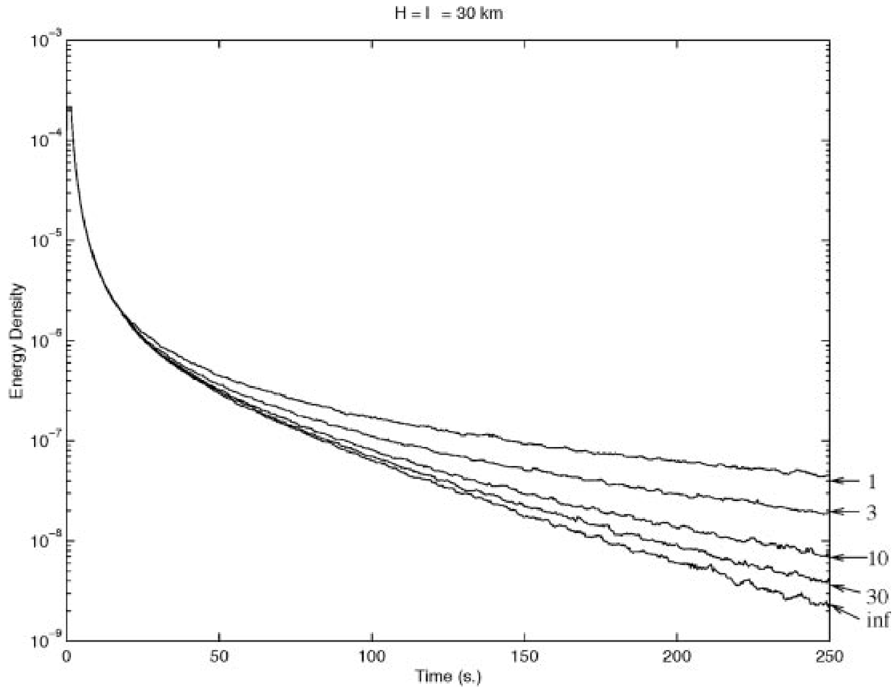


**Figure 4.** Effect of the mean free path contrast on the shape of the synthetic coda. The values of the crustal mean free path $l$ and of the crustal thickness $H$ are indicated at the top of the figure. The ratio of the crustal to the mantle mean free path is indicated beside each curve. There is a steady transition from the algebraic decay, $t^{-3/2}$, when there is no contrast, to the exponential decay, $1/t\,\exp(-t/\tau_d)$, when the mantle is transparent.

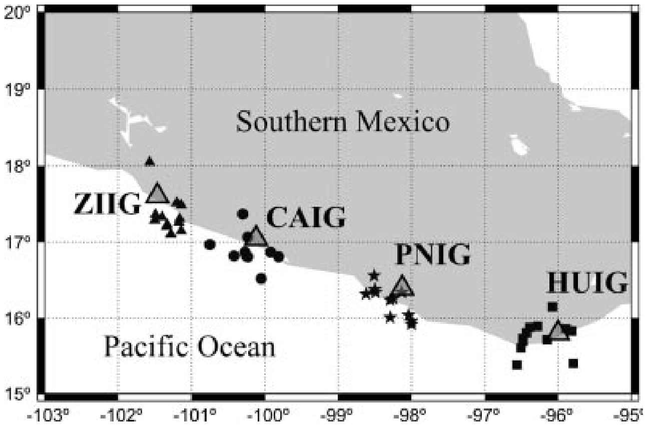


**Figure 5.** Map of epicentre and station locations.

thicknesses $H=20$, 30 km, we plotted the curves corresponding to two extreme sets of model parameters $l$ and $Q_i$, as indicated in the figure. Almost all data points lie between these curves. We note that the values of $Q_i$ necessary to explain the data globally are slightly larger for $H=20$ km than for $H=30$ km. These measurements show the strong frequency dependence of coda $Q$ along the Pacific coast in Mexico and that the conclusions drawn from measurements at CAIG can be extended to the other stations along the coast. Our results indicate the need to take into account the depth dependence of the mean free path and velocity for the interpretation of coda decay in terms of statistical parameters. An interpretation of this data set using a half-space with uniform scattering properties would have led us to infer a large intrinsic absorption at low frequency.

In the preceding analysis, we have used the two crustal thicknesses 20 and 30 km for data interpretation. We emphasize that the values of $H$ used in the model cannot be directly compared to the actual crustal thickness at the station. What matters is the existence of the velocity contrast to create a waveguide, and the *effective* thickness, $H_e$, of the scattering layer. In the continental crust, the heterogeneity is often concentrated in the lower part (see e.g. Fuchs *et al.* 1987; Bois *et al.* 1988). Therefore, in such a case, the thickness of the lower crust could be preferred as the value of $H_e$. Moreover, we stress that it is not possible to neglect the velocity mismatch at the Moho. Even at high frequencies, post-critical reflections at the base of the crust can always be identified on seismograms. We have shown in Paper I that the absence of reflection at the base of the scattering layer would imply a leakage effect much bigger than that observed.

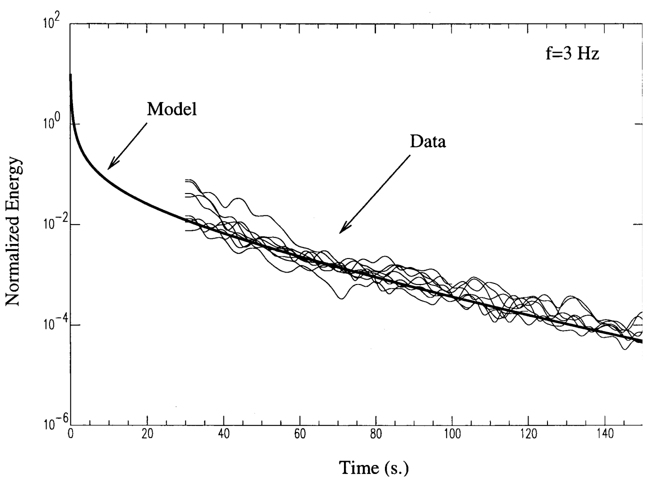


**Figure 6.** Example of smoothed data envelopes from CAIG, filtered around 3 Hz. Data are fitted by assuming $n=1$ in eq. (4). Coda energies are normalized after the individual amplitudes $A^i$ have been determined (see eq. 4). The origin time is the energy release at the source. Note the typical oscillations of individual data envelopes.

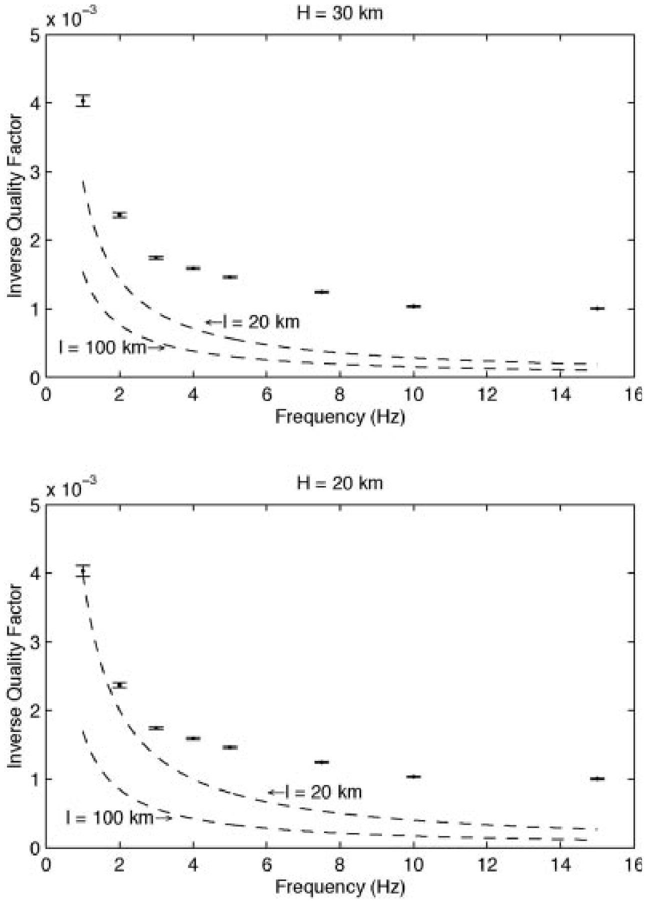


**Figure 7.** Dots with error bars show the values of $1/Q_c$ from 1 to 15 Hz at CAIG. The dashed curves delimit the domain of variation of $1/Q_c^*$ predicted by the model for the crustal thicknesses $H=20$ and 30 km, assuming that $20 < l < 100$ km in the 1–15 Hz frequency band. Arrows show the value of $l$ for each limiting hyperbola.

## 6 IMPORTANCE OF THE LEAKAGE EFFECT

In previous coda studies based on radiative transfer in a uniform half-space, a separation of scattering and intrinsic absorption was proposed. Fehler *et al.* (1992) and Hoshiba (1993) found that $Q_i$ tends to increase with frequency. This would have also been our conclusion if we had based our interpretation on a half-space with constant properties. However, it has been shown that, for the Mexican data, the frequency dependence of $Q_i$ is not required when considering a stratified model including the leakage effect. This shows that the intrinsic $Q$ and the seismic albedo may be underestimated at low

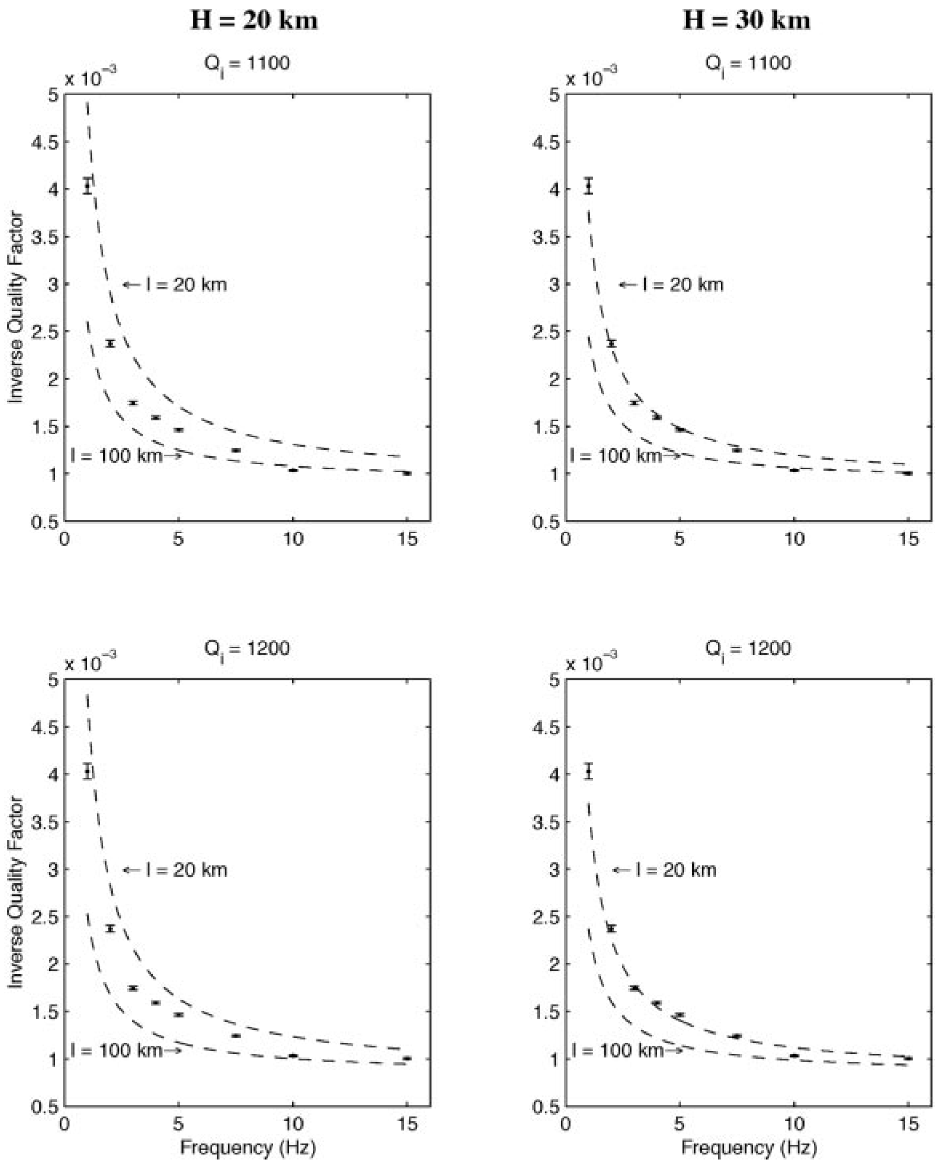


**Figure 8.** Same as Fig. 7 except that a constant intrinsic absorption $Q_i$ has been incorporated in the model. The dashed curves limit the domain of $1/Q_m^*$ predicted by the model for $20 < l < 100$ km.

frequencies (around 1 Hz) when data interpretation is based on uniform half-space models. On the other hand, Fehler *et al.* (1992) and Hoshiba (1993) pointed out that $Q_c$ and $Q_i$ do not differ much at higher frequencies (around 10 Hz), which is in agreement with our interpretation. Therefore, we propose that the intrinsic quality factor of the crust, $Q_i$, can be estimated from the value of $Q_c$ at frequencies larger than about 10 Hz.

In our interpretation we emphasize the effect of leakage. Indeed, we did not demonstrate (nor did we try to do so) that the simple model we propose can be applied everywhere. As already stated, it was found that beneath Japan, $l$ is not much larger in the mantle than in the crust (Aki 1980a,b), implying that the leakage effect is small in this region (Fig. 4). In this case the coda decay is governed by the values of $l$ and $Q_i$ in both the crust and the mantle. In some regions the intrinsic attenuation can be large enough to shadow the leakage effect. This may be the case in Tibet, where the crust is thick and where Kind *et al.* (1996) suggested the presence of partial melting in the crust, which would result in a strong intrinsic attenuation. The low values of $Q_c$ measured by Jin & Aki (1988) in Tibet are in contradiction to the large values expected for a thick crust in our elastic model. In the cases of Japan and Tibet, the leakage effect cannot be the most prominent effect governing the coda decay. It is nevertheless difficult to assess quantitatively its contribution.

On the other hand, in regions where the actual structure of the crust corresponds to the case where $l$ is of the order of $H$, as may be the case in Mexico, $Q_c$ at 1 Hz is determined by the effect of partial leakage of diffuse energy from the scattering crust into the mantle. In this case, the leakage effect is more strongly affected by the variations of $H$ than the variations of $l$, as is clear from Fig. 3 and eq. (3). In regions where $l$ is much larger than $H$, the leakage effect is small. As shown in Fig. 3 for $l = 100$ km, the value of $Q_0^*$ is large and almost independent of the crustal thickness. In this case, we expect $Q_c$ to be mostly determined by absorption. These remarks can be related to the

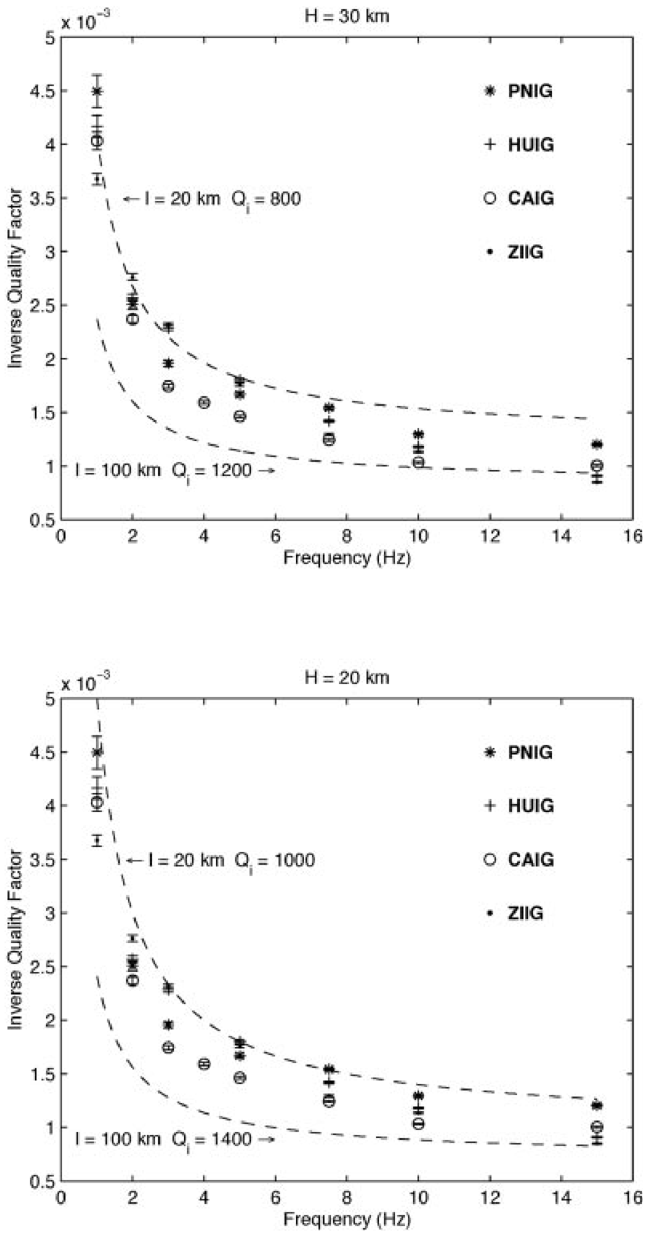


**Figure 9.** Frequency dependence of coda $Q$ at four stations located along the Pacific coast (CAIG, HUIG, PNIG, ZIIG). For each crustal thickness ($H = 20$ and 30 km), we indicate two extreme sets of model parameters $l$ and $Q_i$ such that most data points lie between the curves predicted by the model.

observations of Singh & Herrmann (1983). They showed that in the stable shield areas of North America, where $l$ is supposed to be large, $Q_c$ has high values and is almost frequency-independent, as expected when leakage is negligible. On the other hand, in the tectonically active regions, where $l$ and $H$ may be of the same order, $Q_0$ is of the order of 100–300, and $Q_c$ strongly depends on frequency. Both features support a model where leakage is prominent. When $l$ and $H$ are similar, the decay is strongly sensitive to the crustal thickness. Another parameter, which we did not discuss, is the reflective property of the Moho. Anomalous high velocities in the lower crust would result in a small velocity contrast that enhances the leakage (see eq. 3, where $\xi$ increases with decreasing contrast). This effect can be invoked to explain the measurements of Akamatsu (1990) in Antarctica, which show exceptionally low values of $Q_c$ for a shield.

## 7 CONCLUSIONS

We used a conceptual model of a diffractive crust over a transparent mantle. This model does not represent all conditions in the Earth but it allowed us to demonstrate the importance of the leakage effect due to a contrast between scattering properties of the crust and the mantle. We showed that the interpretation of the coda decay in Mexico does not require a strong intrinsic attenuation, since we found $Q_i$ to be roughly equal to 1000 and almost independent of frequency. The frequency dependence of $Q_c$ is explained by scattering in a stratified model. In fact, the scattering effects tend to dominate at low frequency. A similar conclusion was reached from the study of $L_g$ wave attenuation by Campillo & Plantet (1991). We found a strong sensitivity of the decay rate of the coda with ratio $l/H$. When $l$ is of the order of $H$, the coda decay is more sensitive to a variation of the crustal thickness than of the mean free path. This suggests that, in this condition, the crustal thickness has to be taken into account to interpret the regional variations of coda $Q$. In our modelling, the coda decay at low frequency was governed by the time of residence of diffuse waves in the crust. This model can be applied when a strong mean free path contrast between crust and mantle can be assumed. The model predicts that tectonically active regions (with a small mean free path in the crust) are associated with low values of $Q_c$ at 1 Hz and strong frequency dependence. On the other hand, shields (with a large crustal mean free path) are associated with high values of $Q_c$ and weak frequency dependence.

## ACKNOWLEDGMENTS

We thank K. Aki, M. Hoshiba and G. Müller for their valuable comments and suggestions which helped to improve the manuscript. The authors acknowledge discussions with S. K. Singh, J. Pacheco and C. Bean. The data from stations CAIG, HUIG, PNIG and ZIIG were kindly provided by Servicio Sismologico Nacional, Instituto de Geofisica, UNAM, Mexico. This work was supported by the programmes 'Intérieur de la Terre' of the INSU/CNRS and 'Groupement de Recherches POAN' of the CNRS.

## REFERENCES

Abubakirov, I.R. & Gusev, A.A., 1990. Estimation of scattering properties of lithosphere of Kamchatka based on Monte-Carlo simulation of record envelope of a near earthquake, *Phys. Earth planet. Inter.,* **64,** 52–67.

Akamatsu, J., 1990. Coda attenuation in the Lützow-Holm Bay region, East Antarctica, *Phys. Earth planet. Inter.,* **67,** 65–75.

Aki, K., 1969. Analysis of the seismic coda of local earthquakes as scattered waves, *J. geophys. Res.,* **74,** 615–618.

Aki, K., 1980a. Attenuation of shear-waves in the lithosphere for frequencies from 0.05 to 25 Hz, *Phys. Earth planet. Inter.,* **21,** 50–60.

Aki, K., 1980b. Scattering and attenuation of shear waves in the lithosphere, *J. geophys. Res.,* **85,** 6496–6504.

Aki, K. & Chouet, B., 1975. Origin of coda waves: source, attenuation, and scattering effects, *J. geophys. Res.,* **80,** 3322–3342.

Allmendinger, R.W., Nelson, K.D., Otter, C.J., Barazangi, M., Brown, L.D. & Oliver, J.E., 1987. Deep seismic reflection characteristics of the continental crust, *Geology,* **15,** 304–310.

Bois, C., Cazes, M., Hirn, A., Mascle, A., Matte, P., Montadert, L. & Pinet, B., 1988. Contribution of deep seismic profiling to the knowledge of the lower crust in France and neighbouring areas, *Tectonophysics,* **145,** 253–275.

Campillo, M. & Plantet, J.L., 1991. Frequency dependence and spatial distribution of seismic attenuation in France: experimental results and possible interpretations, *Phys. Earth planet. Inter.,* **67,** 48–64.

Cloves, R.M., Calvert, A.J., Eaton, D.W., Hajnal, Z., Hall, J. & Ross, G.M., 1996. LITHOPROBE reflection studies of Archean and Proterozoic crust in Canada, *Tectonophysics,* **264,** 65–88.

Fehler, M., Hoshiba, M., Sato, H., & Obara, K., 1992. Separation of scattering and intrinsic attenuation for the Kanto-Tokai region, Japan using measurements of S-wave energy vs hypocentral distance, *Geophys. J. Int.,* **108,** 787–800.

Fuchs, K., Bonjer, K.P., Gajewski, D., Lüschen, E., Prodehl, C., Sandmeier, K.J., Wenzel, F. & Wilhelm, H., 1987. Crustal evolution of the Rhinegraben rift by unified geophysical experiments, *Tectonophysics,* **141,** 261–275.

Gusev, A.A., 1995. Vertical profile of turbidity and coda *Q*, *Geophys. J. Int.,* **123,** 665–672.

Hasegawa, H.S., 1985. Attenuation of *Lg* waves in the Canadian shield, *Bull. seism. Soc. Am.,* **75,** 1569–1582.

Herraiz, M. & Espinosa, A.F., 1987. Coda waves: a review, *Pure appl. Geophys.,* **125,** 499–577.

Hoshiba, M., 1993. Separation of scattering attenuation and intrinsic absorption in Japan using the multiple lapse time window analysis of full seismogram envelope, *J. geophys. Res.,* **98,** 15 809–15 824.

Hoshiba, M., 1997. Seismic coda wave envelope in depth dependent S-wave velocity structure, *Phys. Earth planet. Inter.,* **104,** 15–22.

Jin, A. & Aki, K., 1988. Spatial and temporal correlation between coda *Q* and seismicity in China, *Bull. seism. Soc. Am.,* **78,** 744–769.

Kind, R. *et al.*, 1996. Evidence from earthquake data for a partially molten crustal layer in southern Tibet, *Science,* **274,** 1692–1694.

Kostoglodov, V., Bandy, W., Dominguez, J. & Mena, M., 1996. Gravity and seismicity over the Guerrero seismic gap, Mexico, *Geophys. Res. Lett.,* **23,** 3385–3388.

Krishna, V.G., Meissner, R. & Thomas, S.A., 1996. Unusual sub-Moho events near Bornholm, Baltic Sea: modelling of BABEL seismic wide angle data and a tectonic interpretation, *Geophys. J. Int.,* **125,** 193–198.

Margerin, L., Campillo, M. & Van Tiggelen, B.A., 1998. Radiative transfer and diffusion of waves in a layered medium: new insight into coda *Q*, *Geophys. J. Int.,* **134,** 596–612.

McGeary, S. & Warner, M.R., 1985. Seismic profiling the continental lithosphere, *Nature,* **317,** 795–797.

Meissner, R., 1989. Rupture, creep, lamellae and crocodiles: happenings in the continental crust, *Terra Nova,* **1,** 17–28.

Meissner, R., Brown, L., Durbaum, H.J., Franke, W., Fuchs, K. & Seifert, F. (eds), 1990. Continental lithosphere: deep seismic reflections, *Geodyn. Ser.,* Vol. 22, AGU, Washington, DC.

Singh, S. & Herrmann, R.B., 1983. Regionalization of crustal coda *Q* in the continental United States, *J. geophys. Res.,* **88,** 527–538.

Singh, S.K., Pacheco, J., Courboulex, F. & Novelo, D.A., 1997. Source parameters of the Pinotepa Nacional, Mexico, earthquake of 27 March, 1996 (Mw = 5.4) estimated from near-field recording of a single station, *J. Seism.,* **1,** 39–45.

Wu, R.S. & Aki, K., 1988. Multiple scattering and energy transfer of seismic waves: separation of scattering effect from intrinsic attenuation, II, Application of the theory to Hindu Kush region, *Pure appl. Geophys.,* **128,** 49–80.